A Multi-Band/UWB MIMO/Diversity Antenna with an Enhanced Isolation Using Radial Stub Loaded Resonator

Yingsong Li[1], Wenxing Li[1, 2], and Wenhua Yu[1, 2, 3]

[1]College of Information and Communication Engineering,
[2]Institute of Electromagnetic and Wireless Engineering,
Harbin Engineering University, Harbin, Heilongjiang 150001, China
liyingsong82@gmail.com and liwenxing@hrbeu.edu.cn

[3]2COMU, Inc.
State College, PA 16803
wenyu@2comu.com

Abstract **─** In this paper a multi-band/Ultra-Wideband (UWB) Multiple Input Multiple Output (MIMO) antenna, which is composed of two identical microstrip fed triple notch band UWB antennas and a Radial Stub Loaded Resonator (RSLR), is proposed and verified numerically and experimentally. The antenna is designed to meet the requirement of multi-band/UWB communication applications. A Defected Microstrip Structure (DMS) Band-Stop Filter (BSF) and an invert π-shaped slot are employed to design the triple notch band UWB antenna. The resonance characteristics of the DMS-BSF and the band notch functions are presented to realize the proposed triple notch band UWB antenna. The isolation of the multi-band/UWB-MIMO antenna has been enhanced by inserting an RSLR loaded T-shaped stub between two identical triple notch band antennas. Both simulation and measurement results are presented to illustrate the performances of the proposed multi-band/UWB-MIMO antenna.

Index Terms **–** Band notch antenna, diversity antenna, MIMO antenna, multi-band antenna, and UWB antenna.

I. INTRODUCTION

With the rapid development of wireless communication, the high performance modern communication systems with low cost and high data rate have been becoming an urgent requirement. The UWB technology is one of the potential candidates in the race of wireless communication since the Federal Communications Commission (FCC) approved the commercial use of the bandwidth from 3.1 GHz to 10.6 GHz [1]. It is a well-known fact that UWB antenna is one of the key parts in the UWB systems, and many types of UWB antennas have been proposed to meet this application [2-9], such as microstrip fed UWB antenna [2, 4-8] and coplanar waveguide (CPW) fed UWB antenna [3]. However, in contrast to the wide bandwidth of the UWB systems, there exist some Narrow Band (NB) wireless systems that have been licensed and used for a long time. It is necessary to design UWB antenna with notch band characteristic to mitigate the potential interference between NB and UWB systems. Therefore, a practical UWB antenna can not only be satisfying the wide bandwidth, covering the whole UWB band, but also has the low interference with the NB systems. Recently, numbers of UWB antennas including the notch bands have been proposed to reduce the potential interference level [10-16]. However, most of proposed notch band characteristics are obtained by etching various slots on either the radiation patch or the ground plane, which will leak electromagnetic wave, in turn; they will deteriorate the system radiation patterns. In addition, the transmitted power of the UWB systems is limited to a relatively low level (-41.3 dBm/MHz). In order to overcome this limitation, the MIMO technology using multipath

Submitted On: Nov. 9, 2012
Accepted On: Jan. 3, 2013

has been combined with the UWB technology to find an alternative solution for solving the issues above [17-18]. Another challenge in the implementation of the MIMO technique for compact devices arises from the strong mutual coupling between the closely packed antenna elements. Mutual coupling can be usually improved by increasing the distance between the antenna elements but the compact size of the wireless devices makes it impossible in most practical cases [19-27]. A possible approach appears to enhance the isolation or to reduce the mutual coupling by using some other techniques, such as slots and stubs in the antenna structure [19-22]. Furthermore, the DMS structure has been recently widely studied and used for coupling reduction, filter design, and compact antenna design [28-37].

In this paper, a multi-band/UWB-MIMO antenna with anenhanced isolation is proposed and verified numerically and experimentally. The proposed UWB antenna with three notch bands can cover the entire UWB band and also reduce the potential interference from the NB systems. The proposed antenna exploits the approach by using a stub on the ground plane to enhance the isolation. A modified DMS-BSF [31] and an invert π-shaped slot are employed to provide three notch bands for reducing the interference from the NB systems. The mutual coupling between the two multi-band/UWB antennas is reduced by using the RSLR loaded T-shaped stub. The proposed multi-band/UWB-MIMO antenna shows that the isolation level is better than 15 dB over the entire operation band.

Section 2 in this paper presents a triple band notched UWB antenna integrated with the DMS-BSF and the invert π-shaped slot. The resonance characteristic of the DMS-BSF and the notch band functions are analyzed. Moreover, the multi-band/UWB-MIMO antenna with a radial stub loaded resonator loaded T-shaped stub on the ground plane is also proposed. Section 3 illustrates the parametric investigation of the proposed multi-band/UWB-MIMO antenna. The experimental results including the reflection and transmission coefficients, radiation patterns, and the correlation coefficient are presented in section 4. A brief conclusion is presented in section 5.

II. ANTENNA DESIGN

A. Design of the notch band UWB antenna

Figure 1 illustrates the configuration of the proposed triple notch band UWB antenna, which is printed on the substrate surface whose relative dielectric constant, loss tangent, and thickness are 2.65, 0.002, and 1.6 mm, respectively. The UWB antenna consists of a rectangular radiation patch, two square tapped corners at the bottom of rectangular radiation patch, an inverted π-shaped slot embedded in the rectangular radiation patch, a DMS-BSF etched in a microstrip feed line, a partial ground plane, and a 50 Ω microstrip feed line. The radiation patch and the microstrip feed line are printed on the top surface of the substrate while the partial ground plane is printed on the bottom surface. The DMS-BSF embedded in the microstrip feed line is a dual mode resonator, as shown in Fig. 2.

The resonance and phase characteristics of the 50 Ω microstrip line with a meander slot DMS-BSF are shown in Figs. 3 and 4, respectively, in which the parameters L1, g and g1 of proposed DMS-BSF are selected to be 6.6 mm, 0.5 mm, and 0.4 mm, respectively. Figure 3 shows the effects of L1 on the S-parameters of the microstrip feed line with DMS-BSF. It can be observed from Fig. 3 that the DMS-BSF shows dual stop band characteristic in the operation band. As L1 increases, the first resonant frequency shifts down slowly to a lower band while the second resonant frequency moves fast toward a lower band, which means that the length of the meander slot DMS-BSF changes its capacitance characteristic. The first resonant frequency has a tuning stop band from 3.5 GHz to 6 GHz while the second resonant frequency can be adjusted from 7.4 GHz to 12.9 GHz. Therefore, the stop band of the DMS-BSF can be tuned easily. Figure 4 shows the phase characteristic of the microstrip feed line with and without the DMS. A 90º phase jumping for the case with the DMS-BSF is shown in Fig. 4. At frequencies 4.2 GHz and 10.9 GHz, the inductance characteristic changes to be a capacitance in the S21 phase diagram. The discontinuous phase characteristic makes the microstrip line a group delay and two notch bands in the two discontinuous phase points.

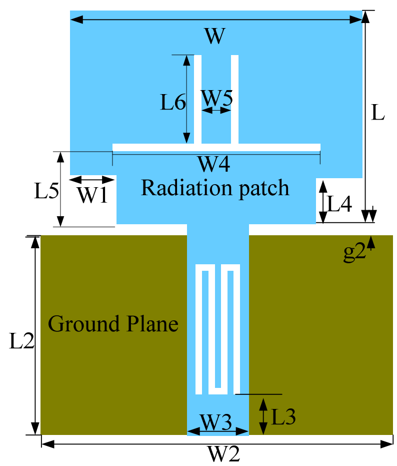

Fig. 1. Geometry of the proposed band notched UWB antenna.

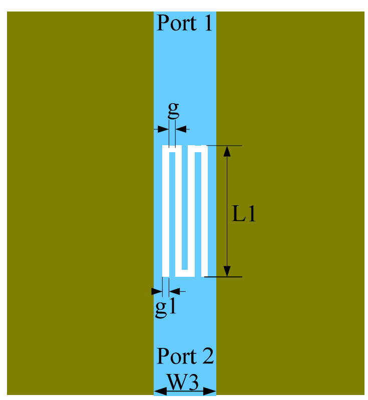

Fig. 2. Structure of the DMS-BSF in the microstrip feed line.

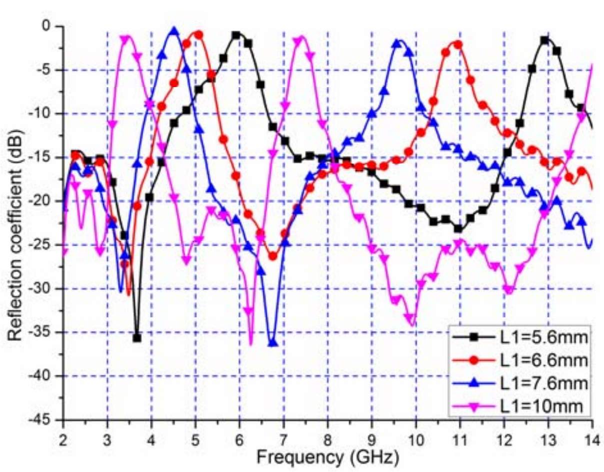

(a)

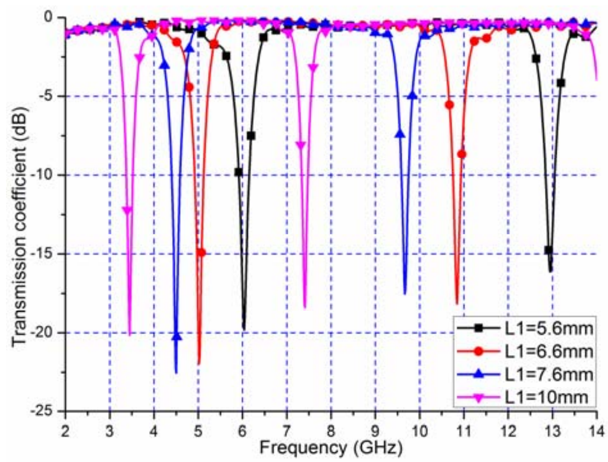

(b)

Fig. 3. Simulated (a) reflection and (b) transmission coefficients of the microstrip feed with DMS-BSF.

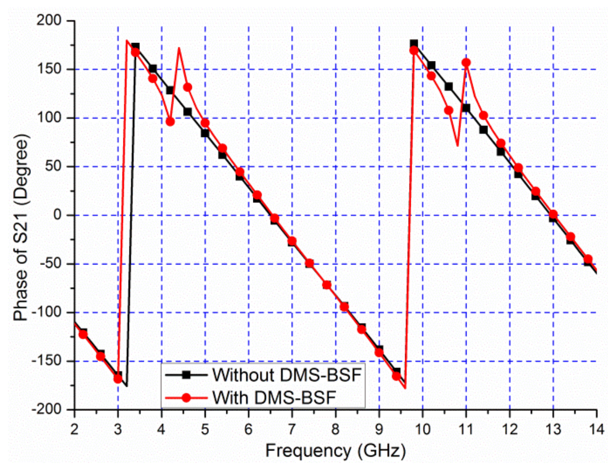

Fig. 4. Phase characteristics of the microstrip feed with DMS-BSF.

Based on the investigation of the microstrip feed line with or without DMS-BSF, another notch band is introduced by using an inverted π-shaped slot etched in the radiation patch. The inverted π-shaped slot is a quarter-wavelength resonant filter. The resonant frequency of the inverted π-shaped slot, for the given dimensions of the notch band function at 6.8 GHz, can also be postulated as,

$$\lambda_{notch} = \frac{c}{f_{notch}\sqrt{\varepsilon_{eff}}} = \frac{c}{f_{notch}\sqrt{\frac{\varepsilon_r + 1}{2}}} \qquad (1)$$

where λ_{notch} is the wave length of the notch band, f_{notch} is the center resonant frequency of the notch band, ε_{eff} is the effective dielectric constant, ε_r is the relative dielectric constant, and c is the speed of light in free space. We take equation (1) in to consideration to achieve the original dimensions of the inverted π-shaped slot in the design. The inverted π-shaped slot is also integrated in the proposed antenna shown in Fig. 1. In order to achieve the ideal simulation results, the proposed tri-notch band UWB antenna is printed on the same substrate with a dielectric constant of 2.65, a loss tangent of 0.002, and a thickness h = 1.6 mm. The simulation results of the tri-notch band functions are shown in Fig. 5.

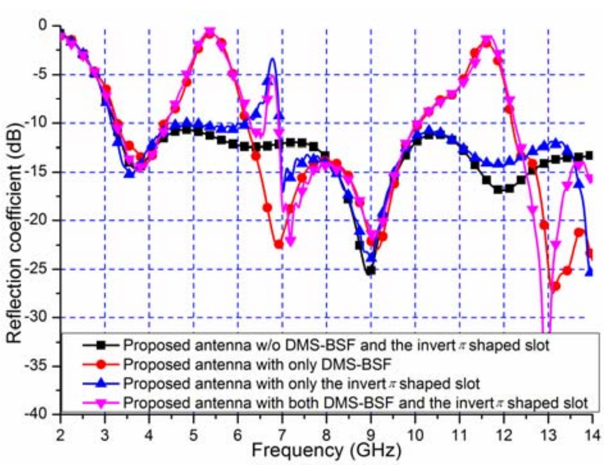

Fig. 5. Reflection characteristics of the proposed tri-notch band UWB antenna.

It can be seen from Fig. 5 that the proposed tri-notch band UWB antenna without the DMS-BSF and the inverted π-shaped slot is an UWB antenna covering the entire band from 3.1 GHz to 14 GHz. When the proposed antenna has only an inverted π-shaped slot, the antenna is an UWB antenna with a notch band near 6.8 GHz, which can reduce the potential interference from RFID systems. As for the proposed UWB antenna with DMS-BSF only, the antenna has two notch bands near 5.5 GHz and 11.5 GHz, respectively. The two notch bands can reduce the potential interference from WLAN, WiMAX, and X-band. The proposed antenna with both DMS-BSF and inverted π-shaped slot has three notch bands. This is also a four band antenna in the frequency bands 3.1 GHz - 4.2 GHz, 6.2 GHz - 6.6 GHz, 7.0 GHz – 10 GHz and 12.2 GHz – 14 GHz. It is observed that the notch band around 6.8 GHz is generated by the inverted π-shaped slot while the other notch bands near the 5.5 GHz and the 11.5 GHz are caused by the DMS-BSF. It is worthwhile to mention that the three notch bands can be designed independently.
The tri-notch band UWB antenna is optimized and fabricated to further verify the proposed design. The optimized dimensions of the proposed tri-notch band antenna are as follow (all units are in mm): L = 15, W = 16, W1 = 2, W2 = 30, W3 = 4.7, W4 = 9, W5 = 3.2, L2 = 16.2, L3 = 3.7, L4 = 2.2, L5 = 4.1, L6 = 6.2, and g2 = 0.8. The parameters L1, g, and g1 of the DMS-BSF are selected to be 6 mm, 0.5 mm and 0.4 mm, respectively. The fabricated tri-notch band UWB antenna is shown in Fig. 6. The measured reflection coefficient, using Anritsu 37347D vector network analyzer, is shown in Fig. 7. It can be observed from Fig. 7 that the measurement results in the low frequency band agree well with the simulated one. The slight discrepancy between the simulated and measured curves in the high frequency band may be caused by the coarse mesh in the numerical simulation using the FDTD method and the fabrication errors.

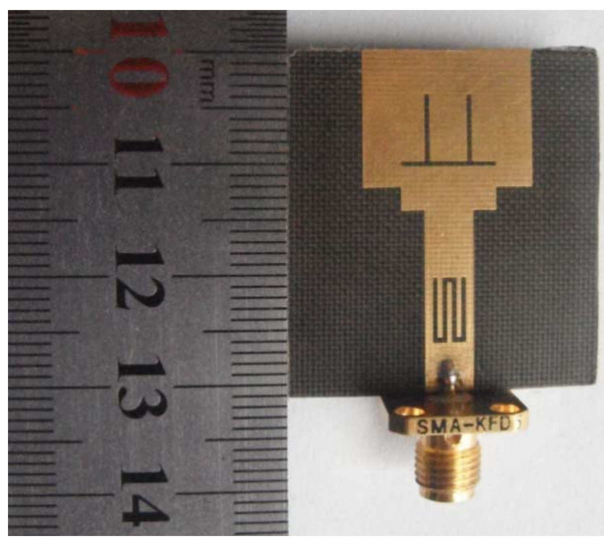

Fig. 6. Photograph of the fabricated tri-notch band antenna.

B. Multi-band/UWB MIMO antenna

In this section, a multi-band/UWB-MIMO antenna is proposed using two identical tri-notch band antennas, as shown in Fig. 8 (a). Based on the investigation of the proposed tri-notch band UWB antenna, the multi-band/UWB-MIMO antenna integrated with an RSLR loaded T-shaped stub is shown in Fig. 8 (c). The RSLR loaded T-shaped stub is illustrated in Fig. 8 (b). The RSLR loaded T-shaped stub is inserted between the two identical tri-notch band UWB antennas in Fig. 8 (a) to form the multi-band/UWB diversity/MIMO antenna shown in Fig. 8 (c).

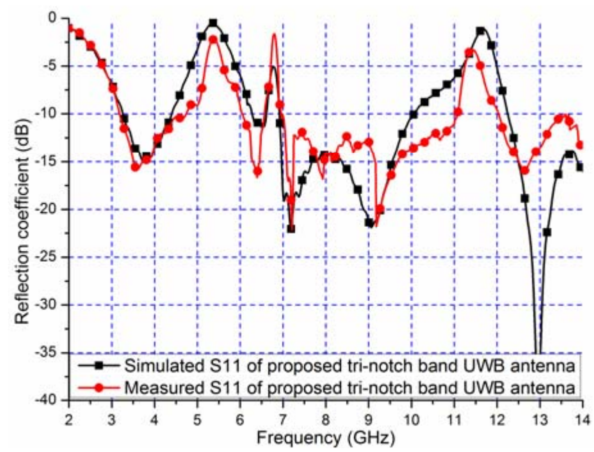

Fig. 7. Measured results of the fabricated tri-notch band antenna.

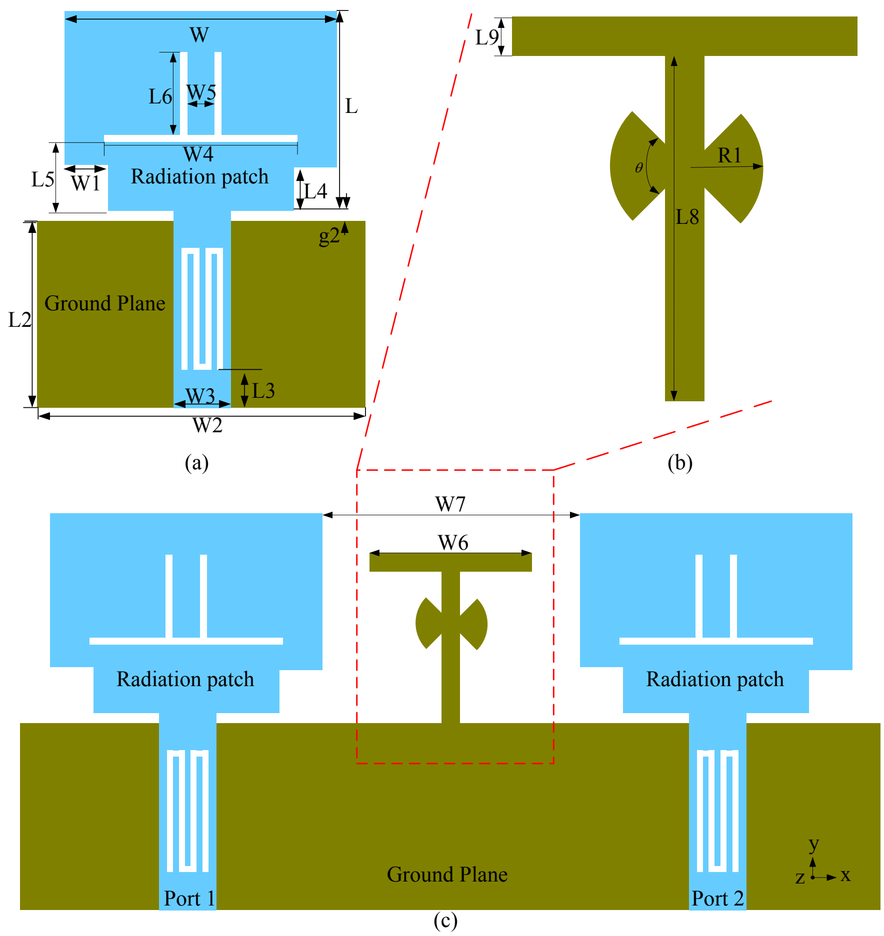

Fig. 8. Geometry of the proposed multi-band/UWB-MIMO antenna.

For the sake of comparison, the multi-band/UWB-MIMO antenna without RSLR loaded T-shaped stub is also investigated to evaluate the performance of multi-band/UWB-MIMO antenna. The multi-band/UWB-MIMO antenna is adjusted to be a smaller size compared with other UWB-MIMO antennas [17-18]. The substrate parameters in the proposed MIMO antennas are selected to be

ε_r = 2.65, δ = 0.002, and h = 1.6 mm. The antenna dimensions are optimized to be (all units are in mm): L = 15, W = 16, W1 = 2, W2 = 30, W3 = 4.7, W4 = 9, W5 = 3.2, L2 = 16.2, L3 = 3.7, L4 = 2.2, L5 = 4.1, L6 = 6.2, g2 = 0.8, W6 = 8, W7 = 14, R1 = 3, L9 = 1, L8 = 9.8, and θ = 60º. The dimensions of the DMS-BSF are selected to be L1 = 6mm, g = 0.5 mm, and g1 = 0.4 mm, respectively.

It is worthwhile to mention that the RLSR loaded T-shaped stub plays a key role in the isolation enhancement. The effects of the RLSR loaded T-shaped parameters on the antenna performance are investigated in the next section. Compared with the stub used in [22], the proposed RSLR loaded T-shaped stub has simple structure and is easy to design.

III. PARAMETRIC STUDY

The proposed RLSR loaded T-shaped stub will be investigated in this section. The reflection and transmission coefficients S_{11} and S_{21}, of the proposed multi-band/UWBMIMO antenna with various parameters are investigated. For the sake of comparison, the multi-band/UWBMIMO antenna without RLSR loaded T-shaped stub is also presented. In the simulation of the multi-band/UWBMIMO antenna, when one parameter changes, the rest of the parameters are kept the same as the optimization parameters listed in section 2. Since the structure is symmetric, it is sufficient to show the S_{11} and S_{21} only. It is observed from the parametric study that the variations of the dimensions of RSLR loaded T-shaped stub are not a linear relationship to S_{11} and S_{21}. The aim of the parametric study is to obtain the variation trend of the S_{11} and S_{21} with the dimension of the RSLR loaded T-shaped stub. The effects of R1, W6, and θ on the antenna performance are presented to investigate S_{11} and S_{21}. The effects of R1 on the antenna performance are demonstrated in Fig. 9. It is found that the impedance bandwidth of the multi-band/UWB MIMO antenna has been improved in the lower frequency band with the increase in the radius R1 of RLSR. The impedance bandwidth between 7 GHz and 9 GHz is deteriorated at a larger radius of RLSR because of the effects on the notch band UWB antennas. The isolation in the lower frequency band has been enhanced significantly with the increase of the radius R1 of RLSR. The isolation between 7 GHz and 9 GHz is a little deteriorated with the increase of R1. This is caused by the increase of R1 near the notch band UWB antenna. Moreover, it also effects the radiation of the proposed multi-band/UWB MIMO antenna elements.

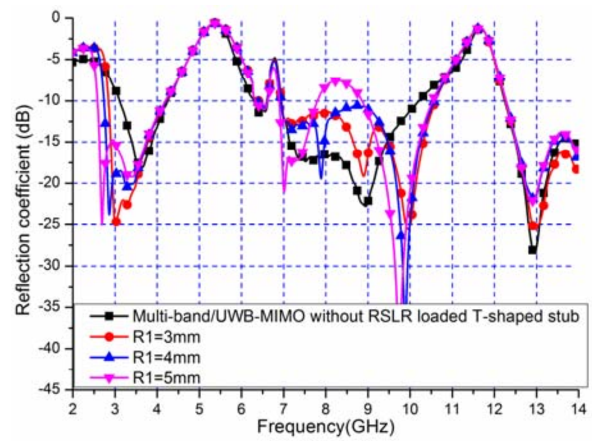

(a)

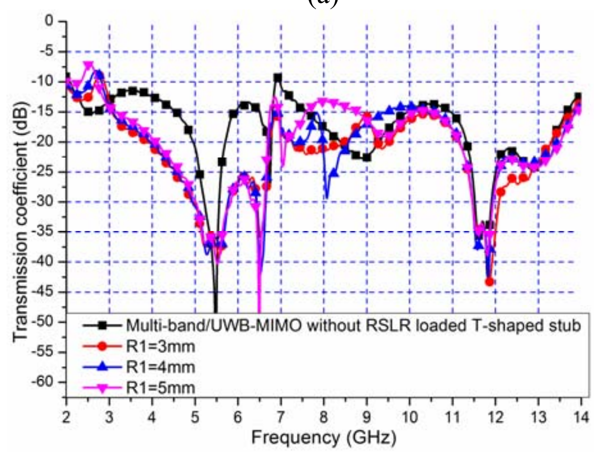

(b)

Fig. 9. Variation of the (a) reflection and (b) transmission coefficients with the parameter R1.

The variation of the S-parameter with θ is presented in Fig. 10. It can be seen from Fig. 10 (a) that the impedance bandwidth at the lower frequency band has been widened with the increase in θ of RLSR. The impedance bandwidth between 8 GHz and 9.3 GHz is getting worse compared with the multi-band/UWB MIMO antenna without RSLR loaded T-shaped stub. It is noticed from Fig. 10 that the bandwidth of the higher notch band near the 11.5 GHz becomes narrower. The isolation shown in Fig. 10 (b) is improved in the lower frequency band. Inside the lower notch band, the isolation at WLAN and WiMAX bands is higher than 25 dB. However, the isolation at the X-band is deteriorated with the increase of parameter θ in RLSR. This is caused by the increase in θ of RLSR near the notch band UWB antenna and the T-shaped stub.

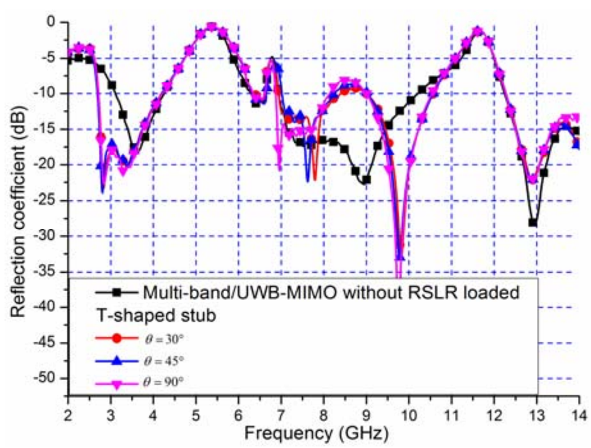

(a)

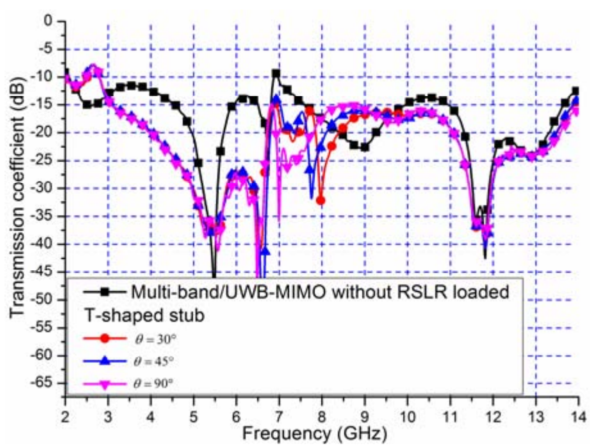

(b)

Fig. 10. Variation of the (a) reflection and (b) transmission coefficients with parameter θ.

The results with W6 variations are summarized in Fig. 11. We can observe from Fig. 11 (a) that the impedance bandwidth of the proposed multi-band/MIMO antenna is increased with W6 while the impedance bandwidth between 7.6 GHz and 8.3 GHz is exacerbated with W6. The bandwidth of the higher notch band is narrower than the proposed MIMO antenna without RSLR loaded T-shaped stub. It is evident that the isolation of the proposed multi-band/MIMO antenna has been improved. The isolation over the entire operation band is better than the MIMO antenna without RSLR loaded T-shaped stub. Especially, in the lower frequency band, the isolation is improved from 5 dB to 10 dB. At 7 GHz, the mutual coupling is reduced about 7 dB for W6 = 6mm. In the high frequency band, the isolation is deteriorated with increasing W6. However, the isolation is improved compared to the MIMO antenna without the RSLR loaded T-shaped stub.

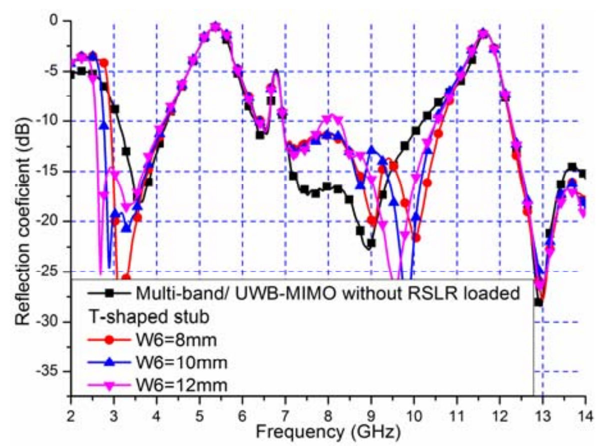

(a)

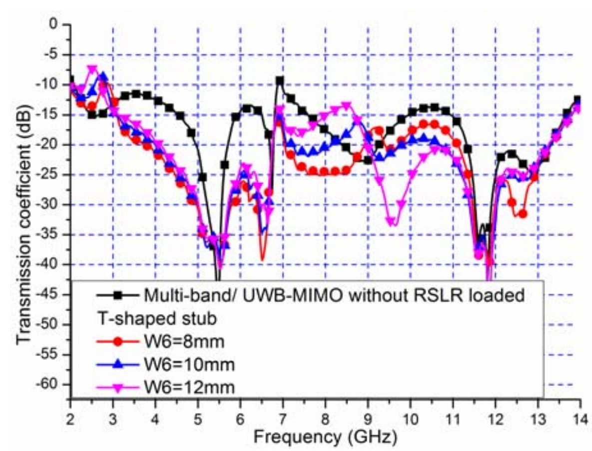

(b)

Fig. 11. Variation of the (a) reflection and (b) transmission coefficients with parameter W6.

The correlation coefficient, which represents the coupling between the antenna elements, is an important parameter in the design of the MIMO antenna. The lower the correlation coefficient is, the better the diversity gain is. The correlation coefficient can be usually calculated from the 3-D radiation patterns generated by exciting different antenna ports or S-parameters. Here, we use the S-parameters to calculate the correlation coefficient based on equation (2), which represents the average correlation between the total powers radiated by the antenna within a 3D space [18],

$$\rho = \frac{\left|S_{11}^{*}S_{12} + S_{21}^{*}S_{22}\right|^{2}}{(1-\left|S_{11}\right|^{2}-\left|S_{21}\right|^{2})(1-\left|S_{22}\right|^{2}-\left|S_{12}\right|^{2})}. \quad (2)$$

There exists an approximate relationship between the diversity gain G_{app} and the correlation coefficient ρ that can be described mathematically [18] as given in equation (3),

$$G_{app} = 10 * \sqrt{1-|\rho|}. \quad (3)$$

According to the investigation aforementioned, the correlation coefficient of the MIMO antenna is shown in Fig. 12. The correlation coefficients are calculated from the S-parameters of the investigated results above. It is found that the correlation coefficient is less than -30 dB except the 6.8 GHz band, as shown in Fig. 12, which corresponds to a high diversity gain. This is due to the proposed RLSR, which can provide a good isolation and thus improves the correlation coefficient. In the RFID band, 6.8 GHz, the correlation coefficient may be attributed to the weak response of the inverted π-shaped slot.

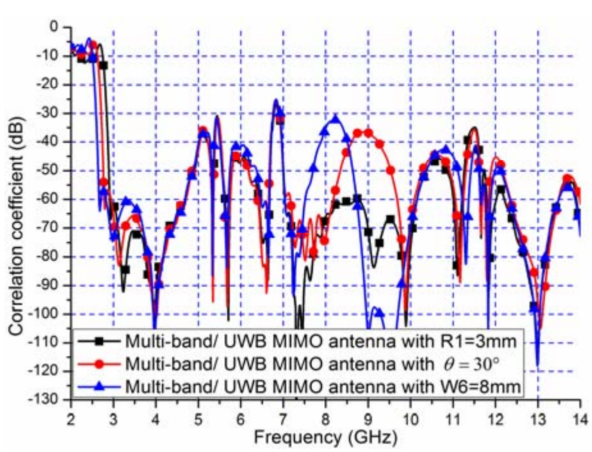

Fig. 12. Correlation coefficient of the proposed multi-band/UWB MIMO antenna.

IV. RESULTS AND DISCUSSIONS

To evaluate the proposed multi-band/UWB MIMO antenna, the designed MIMO antenna is fabricated and measured. The multi-band/UWB MIMO antenna is optimized based on the parametric studies. The geometric parameters are listed as follows (all units are in mm): L = 15, W = 16, W1 = 2, W2 = 30, W3 = 4.7, W4 = 9, W5 = 3.2, L2 = 16.2, L3 = 3.7 L4 = 2.2, L5 = 4.1, L6 = 6.2, g2 = 0.8, W6 = 8, W7 = 14, R1 = 3, L9 = 1, L8 = 9.8, and θ = 60º. The dimensions of the DMS-BSF are L1 = 6mm, g = 0.5mm, and g1 = 0.4 mm. The proposed multi-band/UWB MIMO antenna with the RSLR loaded T-shaped stub is fabricated, as shown in Fig. 13. The measured results are shown in Fig. 14. It can be seen from Fig. 14 that the measured results agree well with the simulated ones. The slight mismatch between the simulated and measured results might be due to the fabrication errors. The measured radiation patterns of the proposed multi-band/UWB MIMO antenna at 3.5 GHz, 6.2 GHz and 9.5 GHz are shown in Fig. 15. In the measurement of the radiation patterns, port 1 is excited while port 2 is terminated with a 50 Ω load. It can be seen from Fig. 15 that the radiation patterns of the proposed multi-band/UWB MIMO antenna are reliable in the operation bands. The patterns in the y-z plane are similar to those in Fig. 15 (a), but not true in the x-z and x-y planes. The difference in the radiation pattern in the x-y plane is useful for pattern diversity as shown in Fig. 15 (a) and (b). In addition, the proposed multi-band/UWB MIMO antenna consists of two identical and symmetric band notched UWB antennas. Therefore, when port 2 is excited and port 1 is matched by a 50 Ω load, the radiation patterns are similar to those shown in Fig. 15.

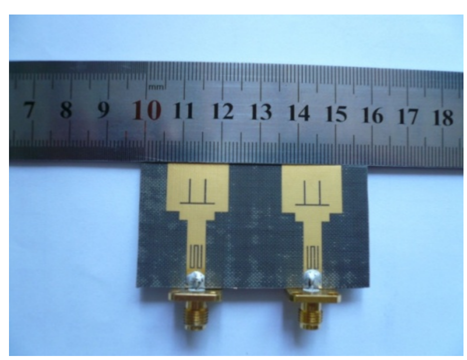

(a)

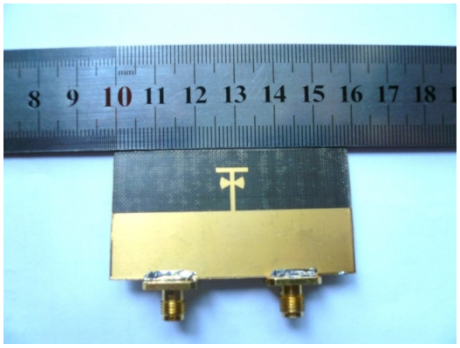

(b)

Fig. 13. Photograph of the (a) front view and (b) back view of the fabricated MIMO antenna.

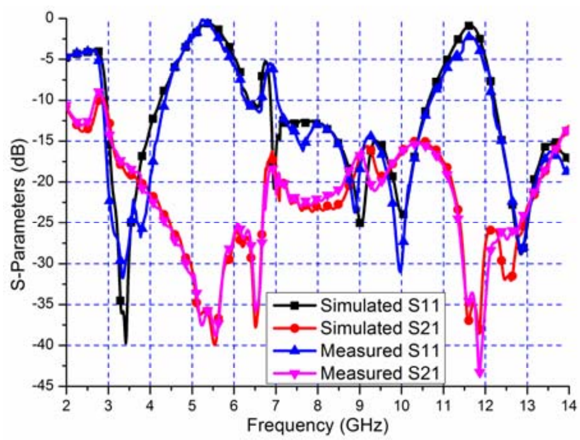

Fig. 14. S-parameters of the proposed multi-band/ UWB MIMO antenna.

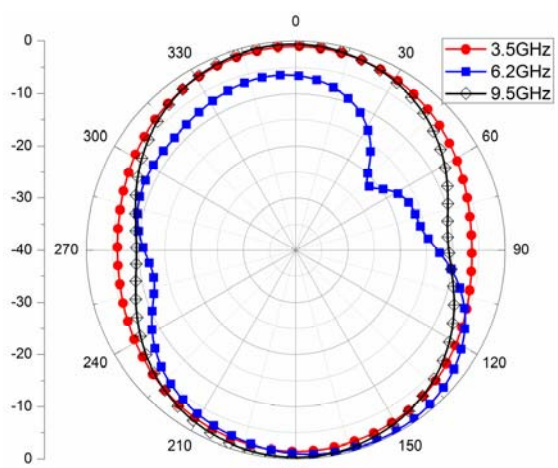

(a) x-z plane

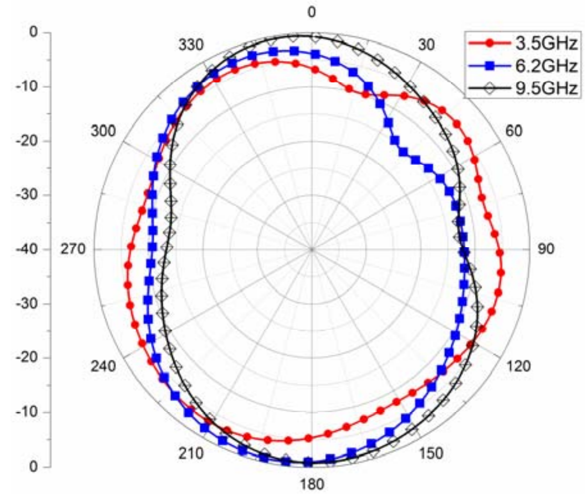

(b) y-z plane

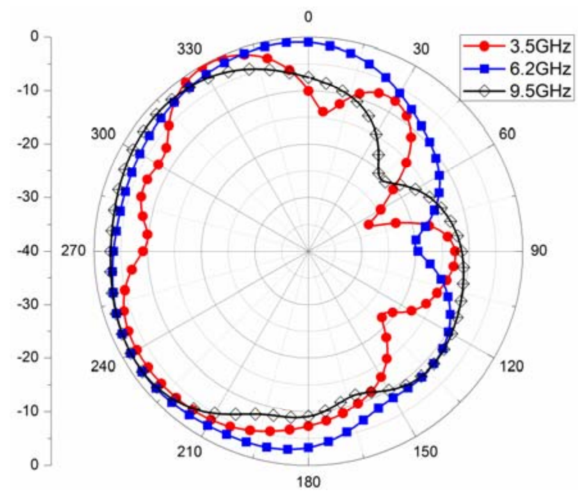

(c) x-y plane

Fig. 15. Radiation patterns of the proposed multi-band/UWB MIMO antenna at different frequencies for the three plane cuts.

The simulated total efficiencies and the maximum absolute gains of the proposed multi-band/UWB MIMO antenna with or without the RSLR loaded T-shaped stub are shown in Figs. 16 and 17, respectively. The proposed antenna has over 80 % efficiency in the operation bands except the notch bands, which are designed for reducing the potential interference between UWB and NB systems [38]. It is evident from Fig. 17 that the efficiency is improved in the lower frequency band. This is caused by the enhanced isolation in the lower frequency band, which reduces the coupling between the two antennas. It can be noticed from Fig. 17 that the gain is reduced in the lower frequency band and that it is similar to that of the design without the RSLR loaded T-shaped stub in the higher frequency band. The variation of the gain is within 2 dBi in the entire frequency band, which is very good for wideband and multi-band systems.

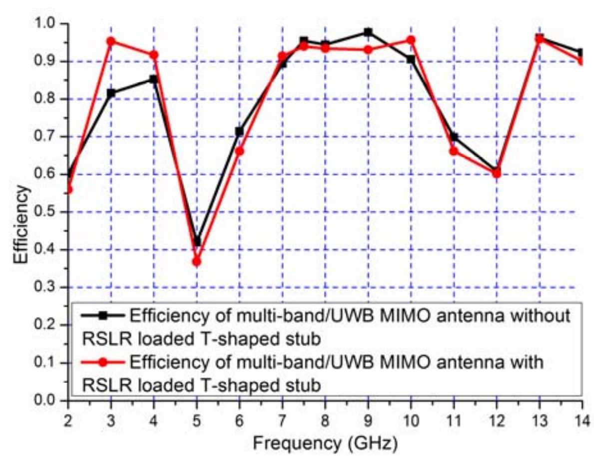

Fig. 16. Efficiency of the proposed MIMO antenna versus frequencies.

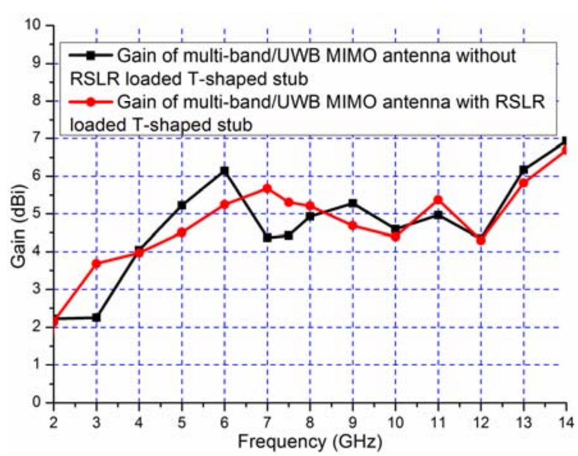

Fig. 17. Gain comparison of the proposed MIMO antenna with and without RSLR loaded T-shaped stub.

V. CONCLUSION

In this paper, a multi-band/UWB MIMO antenna with an RSLR loaded T-shaped stub is investigated numerically and experimentally. The design procedure of the MIMO antenna consists of DMS-BSF, multi-band antenna and RSLR loaded T-shaped stub. The DMS-BSF and RSLR loaded T-shaped stub are employed to generate the band notch characteristics and to increase the isolation of the MIMO antenna, respectively. By adjusting the parameters of the RSLR loaded T-shaped stub, the coupling between the two multi-band/UWB antennas has been reduced. The numerical and experimental results of the impedance bandwidth, isolation level, and radiation patterns demonstrate that the proposed multi-band/UWB MIMO antenna is suitable for multi-band MIMO and UWB MIMO antenna system and other future communication devices. In the future, we will focus on the improvement of the isolation and the design of the reconfigurable MIMO antenna. Such a model of multi-band/UWB MIMO antenna might be constructive for developing universal ultra-wideband MIMO antenna and multi-band MIMO.

ACKNOWLEDGMENT

This paper is also supported by the National Nature Science Fund of China (No.60902014), Nature Science Fund of Heilongjiang (QC2009C66) and the Fundamental Research Funds for the Central Universities (HEUCF1208). The authors are also thankful to Hebei VSTE Science and Technology Co., Ltd. for providing the measurement facility.

REFERENCES

[1] *Federal communications commission, First report and order, Revision of Part 15 of commission's rule regarding UWB transmission system FCC 02-48*, Washington, DC, April 22, 2002.

[2] K. Kiminami, A. Hirata, and T. Shiozawa, "Double-sided printed bow-tie antenna for UWB communications," *Antennas and Wireless Propagation Letters*, vol. 3, pp. 152-153, 2004.

[3] Y. S. Li, X. D. Yang, C. Y. Liu, and T. Jiang, "Compact CPW-fed ultra-wideband antenna with band-notched characteristics," *Electronics Letters*, vol. 46, no. 23, pp. 1533-1534, 2010.

[4] J. Liang, C. C. Chiau, X. Chen, and C. G. Parini, "Study of a printed circular disc monopole antenna for UWB systems," *IEEE Trans. Antennas and Propagation*, vol. 53, no. 11, pp. 3500-3504, 2005.

[5] R. Azim, M. T. Islam, and N. Misran, "Design of a planar UWB antenna with new band enhancement technique," *Appl. Comp. Electro. Society Journal*, vol. 26, no. 10, pp. 856-862, 2011.

[6] S. Sadat, M. Fardis, F. Geran, G. Dadashzadeh, N. Hojjat, and M. Roshandel, "A compact microstrip square-ring slot antenna for UWB applications," *IEEE Int. Symposium Antennas and Propagation Society*, 9-14 July, 2006.

[7] X. L. Bao and M. J. Amman, "Investigation on UWB printed monopole antenna with rectangular slitted ground plane," *Microwave and Optical Technology Letters*, vol. 49, no. 7, pp. 1585-1587, 2007.

[8] D. S. Javan and O. H. Ghouchani, "Cross slot antenna with U-shaped tuning stub for ultra wideband applications," *Appl. Comp. Electro. Society Journal*, vol. 24, no. 4, pp. 427-432, 2009.

[9] Y. Li, W. Li, and R. Mittra, "A cognitive radio antenna integrated with narrow/ultra-wideband antenna and switches," *IEICE Electronics Express*, vol. 9, no. 15, pp. 1273-1283, 2012.

[10] G. Zhang, J. S. Hong, B. Z. Wang, and G. Song, "Switched band-notched UWB/ WLAN monopole antenna," *Appl. Comp. Electro. Society Journal*, vol. 27, no. 3, pp. 256-260, 2012.

[11] Y. Li, W. Li and W. Yu, "A switchable UWB slot antenna using SIS-HSIR and SIS-SIR for multi-mode wireless communications applications," *Appl. Comp. Electro. Society Journal*, vol. 27, no. 4, pp. 340-351, 2012.

[12] R. Fallahi, A. A. Kalteh, and M. G. Roozbahani, "A novel UWB elliptical slot antenna with band-notched characteristics," *Progress In Electromagnetics Research*, vol. 82, pp. 127-136, 2008.

[13] K. S. Ryu and A. A. Kishk, "UWB antenna with single or dual band-notches for lower WLAN band and upper WLAN band," *IEEE Trans. Antennas and Propagation*, vol. 57, no.12, pp. 3942-3950, 2009.

[14] Y. Li, X. Yang, C. Liu, and T. Jiang, "Miniaturization cantor set fractal ultra-wideband antenna with a notch band characteristic," *Microwave and Optical Technology Letters*, vol. 54, no. 5, pp. 1227-1230, 2012.

[15] Y. Kim and D. H. Kwon, "CPW-fed planar ultra wide band antenna having a frequency band notch function," *Electronics Letters*, vol. 40, no.7, pp. 403-405, 2004.

[16] J. Kim, C. S. Cho, and J. W. Lee, "5.2 GHz notched ultra-wideband antenna using slot-type SRR," *Electronics Letters*, vol. 42, no. 6, pp. 315-316, 2006.

[17] A. Najam, Y. Duroc, and S. Tedjni, "UWB MIMO antenna with novel stub structure," *Progress In Electromagnetics Research C*, vol. 19, pp. 245-257, 2011.

[18] M. Jusoh, M. F. Jamlos, M. R. Kamarudin, and F. Malek, "A MIMO antenna design challenges for UWB application," *Progress In Electromagnetics Research B*, vol. 36, pp. 357-371, 2012.

[19] Y. Li, W. Li, C. Liu, and T. Jiang, "A printed diversity cantor set fractal antenna for ultra wideband communication applications," *The 10th Int. Symposium Antenna, Propagation, and EM Theory*, 22-26 October, Xi'an China, 2012.

[20] M. Han and J. Choi, "Dual-band MIMO antenna using a symmetric slotted structure for 4G USB dongle application," *IEEE Int. Symposium Antennas and Propagation (APSURSI)*, 3-8 July, 2011.

[21] Y. Li, W. Li, C. Liu, and T. Jiang, "Two UWB-MIMO antennas with high isolation using sleeve coupled stepped impedance resonators," *Asia-Pacific Conference Antennas and Propagation (APCAP)*, 27-29 August, Singapore, 2012.

[22] S. Zhang, Z. Ying, J. Xiong, and S. He, "Ultra wide band MIMO/diversity antennas with a tree-like structure to enhance wideband isolation," *Antennas and Wireless Propagation Letters*, vol. 8, pp. 1279-1282, 2009.

[23] A. R. Mallahzadeh, S. Es'haghi, and A. Alipour, "Design of an E-shaped MIMO antenna using IWO algorithm for wireless application at 5.8 GHz," *Progress In Electromagnetics Research*, vol. 90, pp. 187-203, 2009.

[24] R. A. Bhatti, J. W. Choi, and S. O. Park, "Quad-band MIMO antenna array for portable wireless communications terminals," *Antennas and Wireless Propagation Letters*, vol. 8, pp. 129-132, 2009.

[25] A. R. Mallahzadeh, S. Es'haghi, and H. R. Hassan, "Compact U-array MIMO antenna designs using IWO algorithm," *Int. Journal of RF and Microwave Computer-Aided Engineering*, vol. 19, no. 5, pp. 568-576, 2009.

[26] S. Zhang, B. K. Lau, Y. Tan, Z. Ying, and S. He, "Mutual coupling reduction of two PIFAs with a T-shape slot impedance transformer for MIMO mobile terminals," *IEEE Trans. Antennas and Propagation*, vol. 60, no. 3, pp. 1521-1531, 2012.

[27] I. Kim, C. Jung, Y. Kim, and Y. Kim, "Low-profile wideband MIMO antenna with suppressing mutual coupling between two antennas," *Microwave and Optical Technology Letters*, vol. 50, no. 5, pp. 1336-1339, 2008.

[28] G. Chaudhary, P. Kim, Y. Jeong, J. Lim, and J. Lee. "Analysis and circuit modeling method for defected microstrip structure in planar transmission lines," *Asia-Pacific Microwave Conference*, pp.999-1002, 2011.

[29] S. Fallahzadeh, H. Bahrami, A. Akbarzadeh, and M. Tayarani, “High-isolation dual-frequency operation patch antenna using spiral defected microstrip structure,” *Antennas and Wireless Propagation Letters*, vol. 9, pp. 122-124, 2010.

[30] M. Kazerooni, A. Cheldavi, and M. Kamarei, “Analysis, modeling, and design of cascaded defected microstrip structure for planar circuits,” *Int. Journal of RF and Microwave Computer-Aided Engineering*, vol. 20, no. 2, pp. 171-181, 2010.

[31] D. La, Y. Lu, and S. Sun, “Novel band stop filter using dual-U shaped defected microstrip structure,” *Int. Symposium Signals, Systems and Electronics*, pp. 1-3, 2010.

[32] M. Naser-Moghadasi, M. Alamolhoda, and B. Rahmati, “Spurious-response suppression in microstrip parallel-coupled bandpass filters by using defected microstrip structures,” *IEICE Electronics Express*, vol. 8, pp. 70-75, 2011.

[33] A. Nouri and G. R. Dadashzadeh, “A compact UWB band-notched printed monopole antenna with defected ground structure,” *Antennas and Wireless Propagation Letters*, vol. 10, pp. 1178-1181, 2011.

[34] S. Zhang, J. K. Xiao, Z. H. Wang, and Y. Li, “Novel microstrip low-pass filters using a defected microstrip structure,” *Microwave Journal*, vol. 49, pp. 118-128, 2006.

[35] H. Cao, W. Guan, S. He, and L. Yang, “Compact lowpass filter with high selectivity using g-shaped defected microstrip structure,” *Progress In Electromagnetics Research Letters*, vol. 33, pp. 55-62, 2012.

[36] J. Wang, H. Ning, L. Mao, and M. Li, “Miniaturized dual-band bandstop filter using defected microstrip structure and defected ground structure,” *IEEE MTT-S International Microwave Symposium Digest (MTT)*, Montreal, QC, Canada, 2012.

[37] D. Cheng, H.C. Yinc, and H.X. Zheng, “A compact dual-band bandstop filter with defected microstrip slot,” *Journal of Electromagnetic Waves and Applications*, vol. 26, no. 10, pp. 1374-1380, 2012.

[38] W. Yu, X. Yang, Y. Liu, et al., *Advanced FDTD Methods: Parallelization, Acceleration and Engineering Applications*, Artech House, 2011,

Yingsong LI received his B.Sc. degree in Electrical and Information Engineering in 2006, and M.Sc. degree in Electromagnetic Field and Microwave Technology from Harbin Engineering University, 2006 and 2011, respectively. Now he is a Ph.D. Candidate in Harbin Engineering University, China. He is a student member of Chinese Institute of Electronics (CIE), IEEE, IEICE and The Applied Computational Electromagnetics Society (ACES). His recent research interests are mainly in microwave theory, small antenna technologies and computational electromagnetics. He serves as reviewers for the journals IEEE Antennas and Wireless Propagation Letters, IEEE Transactions on Electromagnetic Compatibility, Electronics Letters, International Journal of Electronics, Progress In Electromagnetics Research Series, Journal of Electromagnetic Waves and Applications, COMPEL: The International Journal for Computation and Mathematics in Electrical and Electronic Engineering, Wireless Personal communications and Applied Computational Electromagnetics Society Journal. He is also a reviewer of Asia-Pacific Conference on Applied Electromagnetics (APACE2012).

Wenxing LI received the B.Sc. and M.Sc. degrees from Harbin Engineering University, Harbin, Heilongjiang, China, in 1982, 1985, respectively. He is currently a full professor of College of Information and Communication Engineering, Harbin Engineering University, China. He is also the head of Research Centre of EM Engineering & RF Technology. He visited the Department of Electrical Engineering, The Pennsylvania State University, USA from June to August 2010. And he visited Oriental Institute of Technology, Taiwan from August to October, 2010. He is also the organizer of the 30th Progress in Electromagnetics Research Symposium (PIERS), IEEE International Workshop on Electromagnetics (iWEM) , TPC of 2012 Asia-Pacific Symposium on Electromagnetic Compatibility (APEMC 2012) and 2012 Global Symposium on Millimeter Waves (GSMM 2012). His recent research interests are mainly in computational electromagnetic, microwave engineering, modern antenna design and microwave and millimeter wave circuits.

Wenhua Yu joined the Department of Electrical Engineering of the Pennsylvania State University, and has been a group leader of electromagnetic communication lab since 1996. He received his PhD in Electrical Engineering from the Southwest Jiaotong University in 1994. He worked at Beijing Institute of Technology as a Postdoctoral Research Associate from February 1995 to August 1996. He has published one book on CFDTD software and two FDTD books: Conformal Finite-Difference Time-Domain Maxwell's Equations Solver: Software and User's Guide (Artech House, 2003), Parallel Finite-Difference Time-Domain (CUC Press of China, 2005, in Chinese), and Parallel Finite-Difference Time-Domain Method (Artech House, 2006). He has published over 100 technical papers and four book chapters. He developed and created the Computer and Communication Unlimited company (Http://www.2comu.com), and serves as its President. He is a Senior Member of the IEEE. He was included in Who' Who in America, Who' Who in Science and Engineering, and Who's Who in Education. He is also a visiting professor and PhD advisor of the Communication University of China. Dr. Yu's research interests include computational electromagnetic, numerical techniques, parallel computational techniques, and the theory and design of parallel computing systems.